

# Augmented Thrust and Mass Flow Associated with Two-Dimensional Jet Reattachment

T. S. Lund\*

*Joint Institute for Aeronautics and Acoustics, Stanford University, Stanford, California*

An experiment designed to investigate the mass flow and thrust augmentation associated with the flow of a two-dimensional incompressible jet issued parallel to an offset adjacent wall is reported. The results of theoretical development are used to infer both thrust and mass flow augmentation from measured values of the pressure difference across the jet at the exit station. The theory predicts that thrust augmentation is possible only for a wall offset of less than one half of the nozzle exit width. Direct measurements of the mass flow augmentation are in good agreement with the inferred values. Measurements of the separation cavity length are presented that complement those given by previous investigators by extending the range to small values of the ratio of the wall offset to the slot height. For large offset ratios, the cavity length is found to approach a constant fraction of the wall offset distance. The initial radius of curvature of the jet centerline is found to be substantially greater than the mean radius of curvature over the cavity length, thereby indicating that the trajectory of the jet does not follow the arc of a circle, as has been widely assumed.

## Nomenclature

$C_p$	= pressure coefficient
$D$	= base pressure drag per unit span
$h$	= step height; the distance from the reattachment wall to the lower edge of the slot
$J$	= momentum flux per unit span
$\dot{m}$	= exiting mass flux per unit span
$\dot{m}_0$	= exiting mass flux per unit span of an identical jet issued in isolation
$n$	= coordinate normal to the stream direction
$p_b$	= static pressure on the cavity side of the jet at exit
$p_e(y)$	= static pressure profile at the jet exit
$p_T$	= total pressure of the exiting jet
$p_\infty$	= ambient pressure
$R$	= radius of curvature of the jet centerline at the exit station
$Re$	= Reynolds number
$t$	= nozzle slot height
$T$	= thrust per unit span
$T_0$	= thrust per unit span of an identical jet issued in isolation
$u$	= streamwise velocity
$u_e(y)$	= velocity profile at the jet exit
$U$	= velocity magnitude
$x$	= coordinate along the reattachment wall
$x_r$	= jet reattachment point measured from the step
$y$	= coordinate normal to the reattachment wall
$\mu$	= dynamic viscosity
$\rho$	= fluid density
$\phi$	= thrust augmentation ratio

## Introduction

**A**N understanding of the flow characteristics of two-dimensional turbulent jets issued parallel to an offset adjacent wall is important for the utilization of bounded jet flows which

appear in combustion furnaces and reattachment-type fluidic elements. Of equal importance, especially in the design of thrust augmentors used in connection with VSTOL technology, is an understanding of the flowfield generated by a pair of interfering two-dimensional parallel jets. The latter may be studied with a single jet issued parallel to a wall, since experiments<sup>1</sup> have demonstrated that the symmetry plane that exists between the two jets affects the flowfield in much the same way as a solid wall does in the single jet case.

A distinguishing feature of this flow is the presence of a subatmospheric region of separated flow formed between the wall and the curved jet up to the point of reattachment (see Fig. 1). Entrainment of fluid between the jet and the wall serves to lower the pressure in this region and, as a result, the jet curves toward the wall and eventually attaches to it. The jet splits upon merging with the wall and some of its mass is redirected back into the cavity, where it provides a balance for the jet entrainment taking place over the length of the separated region. A stationary vortex within the cavity serves to circulate the flow from the reattachment line back up to the jet shear layer. The pressure within the cavity remains below the ambient value owing to the presence of the vortex.

The conditions of the jet at exit are affected by the presence of the wall since the lowered cavity pressure creates a transverse pressure difference across the jet. In effect, the jet is expanded to a pressure that is lower than atmospheric and, as a consequence, both the exiting mass and momentum flux are increased as compared to an otherwise identical free jet driven by the same total pressure. The increased momentum flux implies an increase in thrust, but the lowered pressure acting over the jet exit and step face creates an opposing force that tends to decrease the overall thrust. The aim of this work is to investigate the prospect of obtaining a net increase in thrust by issuing a plane jet parallel to an offset adjacent wall.

Given that the source of augmented thrust and mass flow is the pressure difference across the exiting jet, it is possible to derive a theoretical relation that allows these quantities to be inferred from measured values of the exit pressure difference across the jet. This approach is preferred over direct measurements of thrust and mass flow not only by virtue of simplicity, but because the magnitude of the increments in mass flow and thrust induced by the presence of the wall are small to the extent that highly accurate instrumentation is

Received Oct. 14, 1985; presented as Paper 85-5002 at the AIAA Third Applied Aerodynamics Conference, Colorado Springs, CO, Oct. 14-16, 1985; revision received April 18, 1986. Copyright © American Institute of Aeronautics and Astronautics, Inc., 1985. All rights reserved.

\*JIAA Research Assistant, Department of Aeronautics and Astronautics, Student Member AIAA.

needed to resolve them. Pressure measurements, on the other hand, are relatively easy to take to the necessary precision with conventional apparatus.

While both the attachment of a jet to an offset parallel plate<sup>1-13</sup> and the interaction of two plane parallel jets<sup>14-17</sup> have been studied extensively in the past, there seems to have been little interest in the aspect of thrust or mass flow augmentation. Newman<sup>3</sup> presented mass flow augmentation measurements for the somewhat related flow of jet reattachment to an inclined wall. Marsters<sup>17</sup> inferred thrust augmentation performance of another related flow consisting of two ventilated interacting plane jets in which a secondary flow was allowed to form between them. No information concerning mass flow or thrust augmentation seems to exist in the literature of the flow presently under consideration.

Many of the previous investigators<sup>1,2,9-13</sup> have provided pressure measurements within the cavity by observing the surface pressure on the wall. Sawyer<sup>1</sup> showed that, excluding the regions close to the exit and reattachment line, the pressure acting across the jet closely follows the wall surface pressure. Such measurements are useful in ascertaining the general trend in the pressure difference across the jet as parameters are varied. The significant departure of the pressure across the jet from the wall surface pressure near the jet exit, however, does not allow the jet exit conditions to be deduced from knowledge of the wall surface pressure.

In the present work, the pressure difference across the jet at the exit station is measured directly. The results of a simple analysis then are used to infer both thrust and mass flow augmentation from these measurements. Mass flow augmentation is also measured directly, and the results are compared with the inferred values in order to validate the analysis. In addition, the length of the separation cavity is investigated by observing the reattachment point. Measurements are taken for a wide range of offset ratios (ratio of the wall displacement from the jet edge to the jet exit width), as well as for various low Mach number jet exit velocities. The jet reattachment point measurements presented here complement those given by previous investigators by extending the range in the low offset ratio regime. Simple scaling laws based on dimensional analysis and incompressible flow theory are developed and tested against the experimental results.

### Dimensional Analysis

The relevant parameters of the problem are the jet stagnation pressure above ambient  $p_T - p_\infty$ , the fluid density  $\rho$ , the dynamic viscosity  $\mu$ , the slot height  $t$ , and the step height  $h$ .

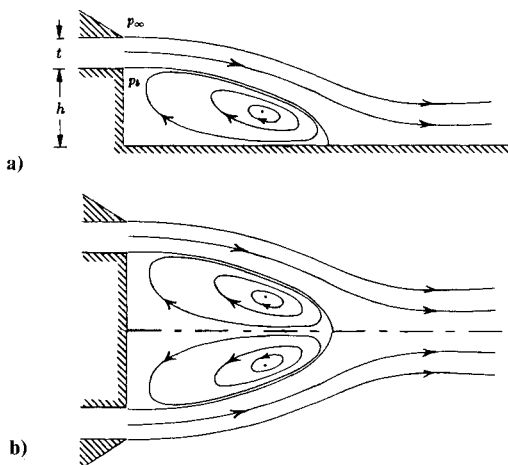


Fig. 1 a) Streamline pattern for a two-dimensional jet issued parallel to an offset adjacent plate (from Ref. 1). b) The flowfield in a) is quite similar to half of the flowfield due to a pair of plane parallel jets, where the symmetry plane between the jets acts like a solid wall.

Any global quantity of interest must depend on these five parameters. Dimensional analysis shows that the nondimensional forms of the jet exit transverse pressure difference, cavity length, jet radius of curvature at exit, and mass flow rate may all be expressed as follows:

$$\frac{p_\infty - p_b}{p_T - p_\infty}, \quad \frac{x_r}{t}, \quad \frac{R}{t}, \quad \frac{\dot{m}}{\dot{m}_0} \sim f\left(R_e, \frac{h}{t}\right) \quad (1)$$

where the Reynolds number is given by

$$R_e = \left(\frac{2(p_T - p_\infty)}{\rho}\right)^{1/2} \left(\frac{t}{\mu/\rho}\right) \quad (2)$$

and the mass flow per unit span of an identical jet issued in isolation is defined as

$$\dot{m}_0 = \left(\frac{2(p_T - p_\infty)}{\rho}\right)^{1/2} (\rho t) \quad (3)$$

If the jet is fully turbulent, it is expected that the flow becomes Reynolds number independent and Eq. (1) will reduce to functions of  $h/t$  alone

$$\frac{p_\infty - p_b}{p_T - p_\infty}, \quad \frac{x_r}{t}, \quad \frac{R}{t}, \quad \frac{\dot{m}}{\dot{m}_0} \sim f\left(\frac{h}{t}\right) \text{ for } R_e \rightarrow \infty \quad (4)$$

When the offset ratio becomes large, it is expected that the flow becomes independent of  $h/t$ , or equivalently, that the relevant length scale to be used in the normalizations becomes  $h$  (and  $t$  leaves the problem). Assuming the offset ratio to be large, Eq. (4) reduces still further to

$$\frac{p_\infty - p_b}{p_T - p_\infty}, \quad \frac{x_r}{h}, \quad \frac{R}{h}, \quad \frac{\dot{m}}{\dot{m}_0} \sim \text{const for } R_e \rightarrow \infty, \quad \frac{h}{t} \gg 1 \quad (5)$$

It is anticipated that the constant that applies to the non-dimensional pressure difference is zero since for very large offset ratios the flow reverts to that of a free jet. By the same reasoning, the constant that applies to the non-dimensional mass flow may be assumed to be unity. The values of the constants which apply to the nondimensional forms of the cavity length and radius of curvature are not obvious and therefore must be determined by the experiment.

### Approximate Analysis for Incompressible Flow

Measurements taken by Sawyer<sup>1</sup> reveal a nearly uniform pressure gradient across the exiting jet. This information suggests that the exit pressure distribution may be described well by a linear profile of the following form:

$$p_e(y) = p_b + (p_\infty - p_b)(y/t + 1/2) \quad (6)$$

The Bernoulli relation, assumed to be valid between the plenum chamber and the jet exit, is given as

$$p_T = p + 1/2 \rho U^2 \quad (7)$$

The exit velocity profile follows from substitution of the assumed exit pressure distribution given by Eq. (6) into the Bernoulli equation

$$u_e(y) = \left\{ \frac{2}{\rho} (p_T - p_\infty) \left[ 1 + \left( \frac{p_\infty - p_b}{p_T - p_\infty} \right) \left( \frac{1}{2} - \frac{y}{t} \right) \right] \right\}^{1/2} \quad (8)$$

### Jet Exit Transverse Pressure Difference

The normal momentum conservation relation for a curved thin jet may be approximated<sup>18</sup> by

$$\frac{\partial p}{\partial n} = \frac{\rho}{R} u^2 \quad (9)$$

This approximate relation is applied at the exit station while making use of the exit velocity profile given by Eq. (8). The resulting expression is integrated over the slot width and simplified to give

$$\frac{p_\infty - p_b}{p_T - p_\infty} = \frac{2(t/R)}{(1 - t/R)} \quad (10)$$

Assuming the radius of curvature to be large compared with the slot height, the above relation may be expanded to give

$$\frac{p_\infty - p_b}{p_T - p_\infty} = 2\left(\frac{t}{R}\right) + \mathcal{O}\left(\frac{t}{R}\right)^2 \quad (11)$$

If the offset ratio  $h/t$  is large, the radius of curvature scales directly with the step height as was shown in Eq. (5). Using this relation in the above expression, the following simplification results

$$\frac{p_\infty - p_b}{p_T - p_\infty} \sim \left(\frac{t}{h}\right)^{-1} \text{ for } \frac{h}{t} \gg 1 \quad (12)$$

### Mass Flow Augmentation

The exiting mass flux per unit span is given as

$$\dot{m} = \rho \int_{-t/2}^{t/2} u_e dy \quad (13)$$

The expression for the exiting velocity profile given by Eq. (8) is expanded for small  $p_\infty - p_b/p_T - p_\infty$  and substituted above to give

$$\dot{m} = \sqrt{2\rho(p_T - p_\infty)} \int_{-t/2}^{t/2} \left\{ 1 + \frac{1}{2} \left( \frac{p_\infty - p_b}{p_T - p_\infty} \right) \left[ \frac{1}{2} - \frac{y}{t} \right] \right\} dy \quad (14)$$

The integration is performed to achieve

$$\dot{m} = \sqrt{2\rho(p_T - p_\infty)} t \left[ 1 + \frac{1}{4} \left( \frac{p_\infty - p_b}{p_T - p_\infty} \right) \right] \quad (15)$$

The mass flow augmentation ratio is formed by normalizing the above relation with the mass flow of an otherwise identical jet issued in isolation [Eq. (3)]

$$\frac{\dot{m}}{\dot{m}_0} = 1 + \frac{1}{4} \left( \frac{p_\infty - p_b}{p_T - p_\infty} \right) \quad (16)$$

### Thrust Augmentation

The momentum flux of the exiting jet is defined as

$$J = \rho \int_{-t/2}^{t/2} u_e^2 dy \quad (17)$$

The expression for the exiting jet velocity profile given by Eq. (8) is substituted above, and the integration performed to yield

$$J = 2(p_T - p_\infty) t \left[ 1 + \frac{1}{2} \left( \frac{p_\infty - p_b}{p_T - p_\infty} \right) \right] \quad (18)$$

In computing the thrust, the pressure force acting over the slot and step face must be taken into account. For simplicity, the assumption is made that the pressure acting over the step face is constant and equal to the base pressure  $p_b$ . With this assumption, the drag force may be written as

$$D = (p_\infty - p_b) h + \int_{-t/2}^{t/2} (p_\infty - p_e) dy \quad (19)$$

The integration is performed with aid of the exit pressure profile given by Eq. (6) and the resulting expression rearranged to read

$$D = (p_T - p_\infty) t \left( \frac{p_\infty - p_b}{p_T - p_\infty} \right) \left[ \frac{1}{2} + \left( \frac{h}{t} \right) \right] \quad (20)$$

The thrust now can be obtained by subtracting the base pressure drag from the momentum flux:

$$T = J - D = 2(p_T - p_\infty) t \left\{ 1 + \frac{1}{2} \left( \frac{p_\infty - p_b}{p_T - p_\infty} \right) \times \left[ \frac{1}{2} - \left( \frac{h}{t} \right) \right] \right\} \quad (21)$$

The thrust produced by an identical nozzle issued in isolation is found from the above relation by setting the exit transverse pressure difference  $p_\infty - p_b/p_T - p_\infty$  to zero. This done, the thrust augmentation ratio is readily formed

$$\phi \equiv \frac{T}{T_0} = 1 + \frac{1}{2} \left( \frac{p_\infty - p_b}{p_T - p_\infty} \right) \left[ \frac{1}{2} - \left( \frac{h}{t} \right) \right] \quad (22)$$

An immediate observation from this result is that a net gain in thrust can be achieved only if the offset ratio is less than one half.

### Experimental Apparatus

A cross-sectional view of the experimental arrangement is shown in Fig. 2. Air flows from a mechanical blower, through a mass flow meter, and into the plenum chamber, where the total pressure is measured just upstream of the nozzle contraction. In an effort to reduce rounding of the exit velocity profile, the boundary layers that develop over the length of the contraction are tripped just prior to the

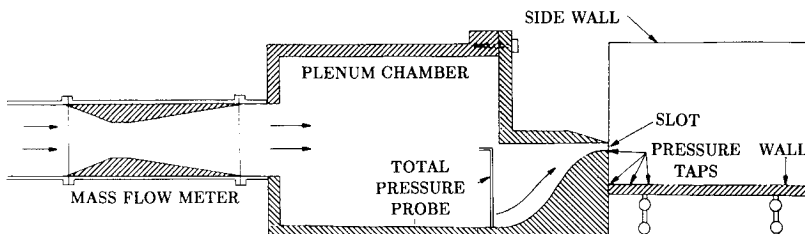


Fig. 2 Experimental configuration. The span is 5 cm and the reattachment wall extends three span lengths downstream.

nozzle exit by means of sandpaper strips adhered to the upper and lower walls. The nozzle is aligned to be parallel to the offset wall and a pair of side plates are employed to preserve the two-dimensional conditions downstream of the nozzle. Both the slot height and the step height may be varied independently to give a wide range of offset ratios. The transverse pressure difference across the jet is measured via a pressure tapping located at midspan on the step face immediately below the jet exit. Additional pressure tappings are provided along the reattachment wall so that the static pressure distribution there also may be observed.

The reattachment point is observed through the use of an oil flow technique in which a suspension of titanium dioxide is painted along the reattachment wall. Once the flow has been established, a spanwise line of particles delineates the reattachment point. Use of the oil flow also provides a means to ascertain the extent to which the flow is two-dimensional.

The flow was found to be Reynolds number independent for Reynolds numbers greater than  $2 \times 10^4$ . All measurements were taken in the Reynolds number range  $2-5 \times 10^4$ . For each offset ratio, pressure difference measurements were taken at several values of the total pressure and the nondimensional pressure differences were then averaged.

Direct measurements of the mass flow augmentation were created by forming the ratio of the observed mass flow rates, taken at the same total pressure, with and without the reattachment wall. Some difficulty was encountered in taking these measurements since the difference in mass flow with and without the wall was on the order of a few percent while the repeatability of the readings was about one half of a percent. In an effort to help resolve the small increments in mass flow from the noise of the instrumentation, 10-15 readings were taken at each offset ratio and the results then averaged. With this sample size, the standard deviation of a series of measurements was typically 0.002.

The measurements were taken at nozzle aspect ratios of both 10 and 18. Figure 3 shows a typical oil flow pattern for an aspect ratio of 10. It can be seen that the presence of the side walls introduces some three-dimensional effects as the reattachment line is bent back toward the slot near the edges. It may be assumed that near midspan the effects of the side walls have become negligible and the conditions are more nearly two-dimensional. All measurements were taken at the midspan station.

Results and Discussion

Jet Exit Transverse Pressure Difference

Measurements of the pressure difference across the jet at the exit station are displayed in Table 1 and Fig. 4. For comparison, data due to Sawyer,<sup>1</sup> as well as the mean pressure

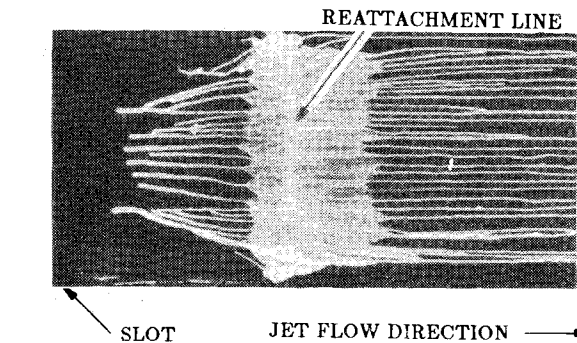


Fig. 3 Typical oil flow pattern for a nozzle aspect ratio of 10 and  $h/t=3.25$ . The reattachment point is visible as the solid thin lateral white line. Note that the conditions are not entirely two-dimensional, but spanwise variations near the center where the measurements are made are small.

within the cavity as reported by Nozaki et al.,<sup>10</sup> are plotted with the present results. Sawyer's data, deduced from his detailed map of the pressure within the cavity, is seen to be in satisfactory agreement with the present data. It is evident that except for small offset ratios, the mean suction within the cavity is greater than that at the exit station. Both the mean cavity pressure and the initial pressure difference across the jet exhibit a similar break point at a moderate offset ratio where it appears that a readjustment of the flow within the cavity is taking place. For the purpose of further analysis, the present data has been fitted to the following relations. For small offset ratios

$$\frac{p_{\infty}-p_b}{p_T-p_{\infty}}=(0.125\pm0.64\%)\left(\frac{h}{t}\right)^{(-0.309\pm0.998\%)}$$

for  $0.194\leq\frac{h}{t}\leq3.42$

(23)

with a correlation coefficient of 0.984 and for large offset ratios

$$\frac{p_{\infty}-p_b}{p_T-p_{\infty}}=(0.343\pm22.0\%)\left(\frac{h}{t}\right)^{(-1.13\pm10.9\%)}$$

for  $3.42\leq\frac{h}{t}\leq21.3$

(24)

with a correlation coefficient of 0.944. Note that for large offset ratios the exponent in Eq. (24) is close to  $-1$  as predicted by the result of the dimensional analysis given in Eq. (12).

Reattachment Wall Static Pressure Distribution

The wall static pressure distribution for several offset ratios is displayed in Fig. 5. For this purpose, the pressure coefficient is defined as

$$C_p=p-p_{\infty}/p_T-p_{\infty}$$

(25)

Table 1 Jet exit transverse pressure difference measurements<sup>a</sup>

$\frac{h}{t}$	$\frac{p_{\infty}-p_b}{p_T-p_{\infty}}$	$\frac{h}{t}$	$\frac{p_{\infty}-p_b}{p_T-p_{\infty}}$
0.194	0.200	1.05	0.118
0.327	0.178	1.13	0.117
0.377	0.162	1.13	0.128
0.409	0.164	1.34	0.117
0.450	0.171	1.62	0.114
0.471	0.156	1.62	0.111
0.491	0.150	2.07	0.0958
0.491	0.157	2.59	0.0918
0.524	0.152	3.24	0.0829
0.567	0.154	3.25	0.0675
0.573	0.150	3.94	0.0705
0.576	0.148	4.72	0.0545
0.648	0.139	4.78	0.0468
0.654	0.143	4.93	0.0603
0.681	0.137	5.90	0.0574
0.736	0.135	6.40	0.0454
0.786	0.132	6.53	0.0502
0.810	0.135	7.08	0.0538
0.891	0.133	7.14	0.0367
0.926	0.132	7.88	0.0327
0.943	0.126	10.2	0.0249
0.995	0.124	12.3	0.0178
1.01	0.132	14.9	0.0205
0.01	0.119	21.3	0.0076

<sup>a</sup>Bold entries are for nozzle aspect ratio 18, all other points for nozzle aspect ratio 10.

It is observed that the pressure within the cavity is not constant over its length, but rather the suction increases in magnitude from the nozzle to a point close to reattachment. At this point, there is a fast pressure recovery zone followed by a relaxation to the ambient value after reattachment. It also appears that the pressure distribution is losing its dependence on the offset ratio as the latter becomes large.

Cavity Length

Measured reattachment distances are tabulated in Table 2 and plotted along with those provided by previous investigators in Fig. 6. The present data are in close agreement with the previous measurements for the entire range of offset ratios. Also shown in Fig. 6 is a theoretical curve due to Bourque,<sup>7</sup> which provides a good correlation with the data except at the very smallest offset ratios. Other theories (cf. Bourque and Newman,<sup>2</sup> Sawyer,<sup>1,4</sup> and Perry<sup>8</sup>) do not fit the data as well as Bourque's theory of 1967.

As was shown in the previous section on dimensional analysis, the cavity length should approach a constant fraction of the step height as the offset ratio becomes large [see Eq. (5)]. This constant is determined by replotting the data of Fig. 6 so that the cavity length, now normalized by the step height, is plotted against the inverse of the offset ratio, as shown in Fig. 7. An infinitely large offset ratio is mapped to the origin, and the desired constant is found as the point at which a curve fit through the data intersects the  $x_r/h$  axis. A linear regression is used for data taken at offset ratios greater than 4. The resulting value of the constant is found to be

$$\frac{x_r}{h} = 1.25 \pm 4.64\% \text{ for } \frac{h}{t} \gg 1 \tag{26}$$

Mass Flow Augmentation

Measured values of the mass flow augmentation are shown in Table 3 and plotted in Fig. 8, along with the computed

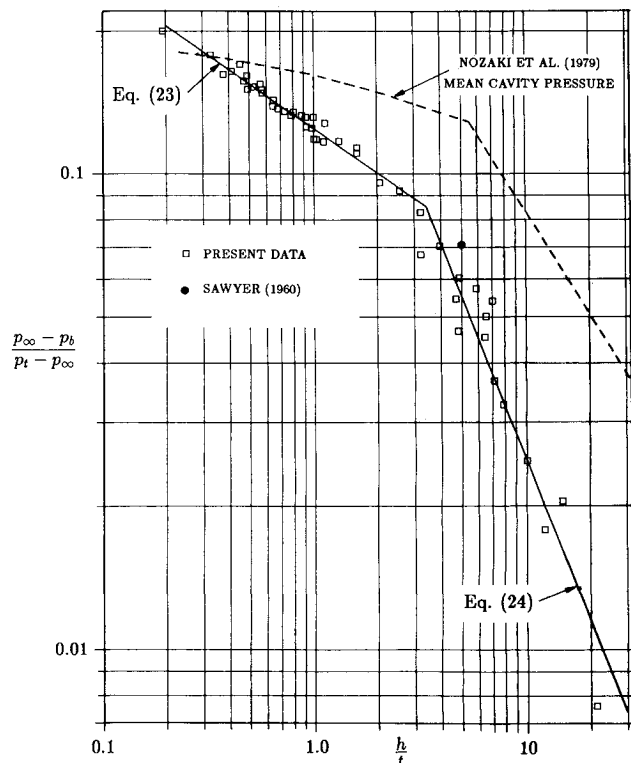


Fig. 4 Jet exit transverse pressure difference. Measurements taken both at nozzle aspect ratio 10 and 18 show no systematic dependence on aspect ratio. Sawyer's datum<sup>1</sup> was found from a detailed pressure map of the separation cavity.

values generated by substituting the curve-fit expression for the transverse exit pressure difference given by Eqs. (23) and (24) into the theoretical expression of Eq. (16). The agreement is satisfactory over the range of the measurements. The good correlation between the inferred and measured values suggests that the assumed linear pressure profile at the jet exit is a valid approximation and therefore provides a justification for the use of the present analysis.

Thrust Augmentation

Thrust augmentation is inferred from the exit transverse pressure difference by combining the curve-fit expression given by Eq. (23) with the theoretical expression for the thrust augmentation ratio given by Eq. (22). The resulting expression,

$$\phi = 1 + \frac{1}{2} \left[ 0.125 \left( \frac{h}{t} \right)^{-0.309} \right] \left[ \frac{1}{2} - \left( \frac{h}{t} \right) \right] \tag{27}$$

is plotted in Fig. 9. As pointed out in the analysis, thrust augmentation exists only for offset ratios of less than one half.

Table 2 Cavity length measurements<sup>a</sup>

$h/t$	$x_r/t$	$h/t$	$x_r/t$
0.194	0.969	1.34	4.90
0.327	1.44	1.41	5.36
0.377	1.98	1.62	5.71
0.409	2.04	1.97	6.40
0.450	2.10	2.07	6.83
0.471	2.27	<b>2.36</b>	<b>7.96</b>
0.491	2.37	2.59	7.85
0.491	2.32	<b>3.20</b>	<b>10.5</b>
0.524	2.37	3.24	8.98
0.567	2.65	3.25	8.73
0.573	2.47	<b>3.28</b>	<b>8.23</b>
0.576	2.47	<b>3.54</b>	<b>10.4</b>
0.648	2.96	3.94	9.99
0.654	2.80	<b>4.18</b>	<b>11.8</b>
0.681	2.78	<b>4.72</b>	<b>12.6</b>
0.736	3.40	<b>4.78</b>	<b>12.9</b>
0.786	3.20	4.93	11.8
0.810	3.47	<b>5.90</b>	<b>14.1</b>
0.891	3.67	6.40	14.4
0.943	3.92	<b>6.53</b>	<b>15.2</b>
0.995	4.12	7.14	15.3
<b>1.01</b>	<b>3.77</b>	7.88	16.3
1.05	4.33	<b>10.2</b>	<b>21.2</b>
1.13	4.43	12.3	21.9
1.13	4.33	<b>14.9</b>	<b>26.5</b>
<b>1.18</b>	<b>3.88</b>	<b>21.3</b>	<b>35.8</b>
1.26	4.84		

<sup>a</sup>Bold entries are for nozzle aspect ratio 18, all other points for nozzle aspect ratio 10.

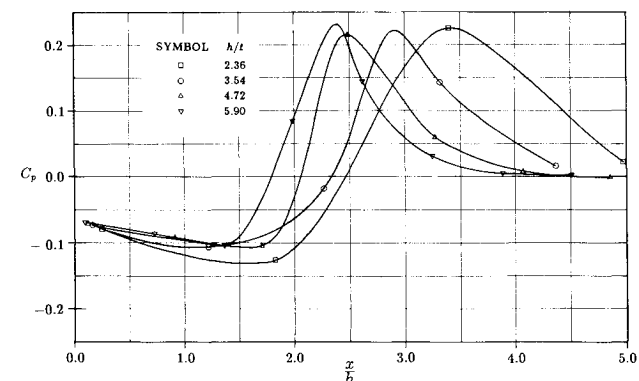


Fig. 5 Reattachment wall static pressure distribution. Measurements are taken at a nozzle aspect ratio of 18.

The presence of thrust augmentation suggests that an increase in thrust may be realized by splitting a standard single two-dimensional jet nozzle into two plane parallel jets issuing in close proximity to each other. There will exist an optimal spacing between the jets, where the thrust augmentation is maximized. A maximum will occur since the pressure difference across the jet must vanish for zero offset ratio. Due to the limitations of the experimental apparatus, the location of the maximum initial pressure difference across the jet could not be determined and is presumed to lie at an offset ratio of less than 0.2. This fact also suggests that thrust augmentation in excess of 3% may be present at the optimal offset ratio. Future work in this area should focus on the low offset regime, and in particular, in identifying the offset ratio at which the initial pressure difference is maximized.

Initial Radius of Curvature of the Jet Centerline

It is interesting to consider the radius of curvature of the jet centerline, since most theories that predict the cavity length and the mean cavity pressure need to assume the shape of the jet trajectory. The initial radius of curvature of the jet centerline may be inferred from the jet exit transverse pressure difference by rearranging Eq. (10)

$$\frac{R}{t} = 1 + \left[ 2 / \left( \frac{p_{\infty} - p_b}{p_T - p_{\infty}} \right) \right] \tag{28}$$

Use of the curve fit expression for  $p_{\infty} - p_b / p_T - p_{\infty}$  given by Eqs. (23) and (24) in the above expression allows the curve shown in Fig. 10 to be generated. Also shown in Fig. 10 are the mean radii of curvature found by previous investigators. The curve due to Nozaki et al.<sup>10</sup> was generated by the author from their mean cavity pressure measurements. The curve due to Tanaka<sup>15</sup> is a direct measurement of the mean curvature for a dual jet flow.

Note that the initial radius of curvature of the jet centerline is substantially larger than the mean radius of curvature. This observation is important because it shows that the path of the jet is not the arc of a circle as has been

Table 3 Mass flow augmentation measurements<sup>a</sup>

<i>h</i> / <i>t</i>	$\dot{m}/\dot{m}_0$	<i>h</i> / <i>t</i>	$\dot{m}/\dot{m}_0$
0.974	1.0305	2.82	1.0175
1.31	1.0273	3.03	1.0199
1.49	1.0249	3.49	1.0150
2.03	1.0255	4.15	1.0120
2.62	1.0226	5.13	1.0108
2.72	1.0204	6.15	1.0093

<sup>a</sup>All values are for nozzle aspect ratio 10.

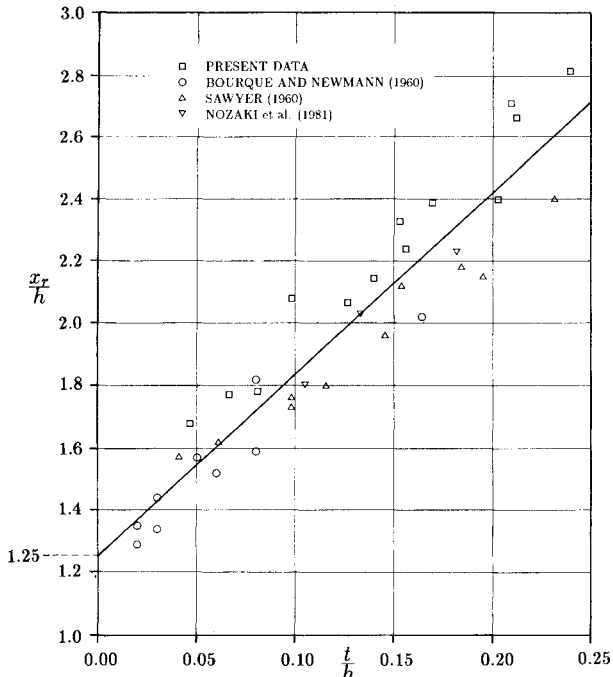


Fig. 7 Rescaling of the cavity length measurements. The asymptotic behavior of the cavity length for large offset ratios is determined as the intercept of the best fit through the data with the  $x_r/h$  axis.

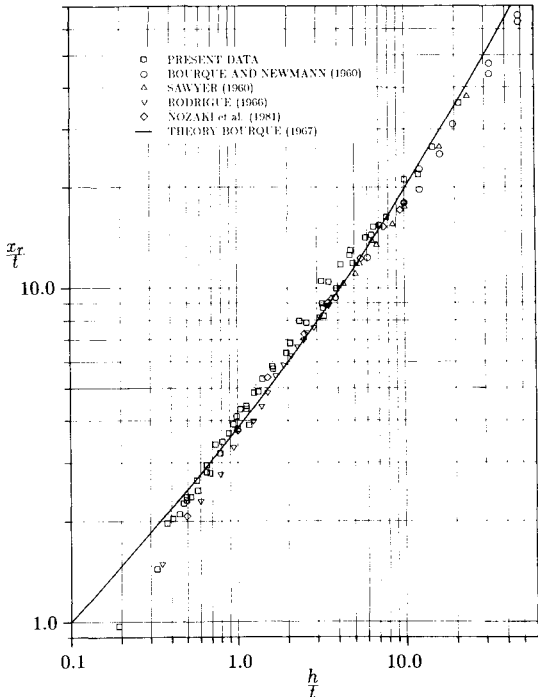


Fig. 6 Cavity length. Measurements taken both at nozzle aspect ratio 10 and 18 show no systematic dependence on aspect ratio. Where necessary, the measurements taken by previous investigators have been rescaled to be consistent with the present normalizations.

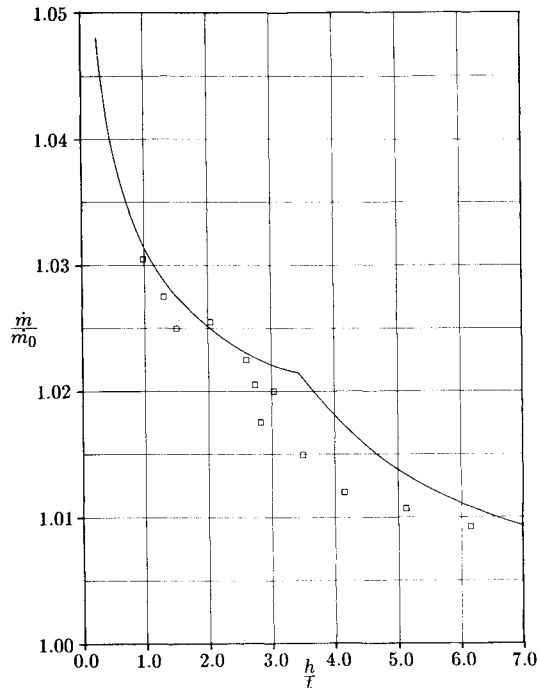


Fig. 8 Mass flow augmentation. The solid curve is obtained from the theoretical expression of Eq. (16) combined with the heuristic expressions for the initial pressure difference across the jet given by Eqs. (23) and (24).

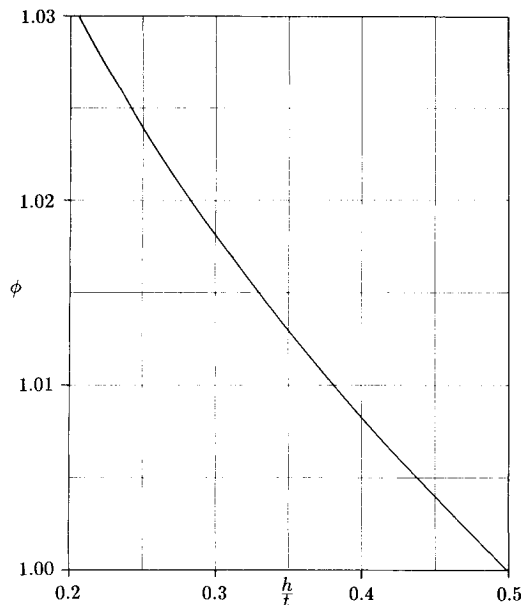


Fig. 9 Thrust augmentation. Plot of Eq. (27) for the augmented thrust predicted by the theory and the jet exit pressure difference measurements.

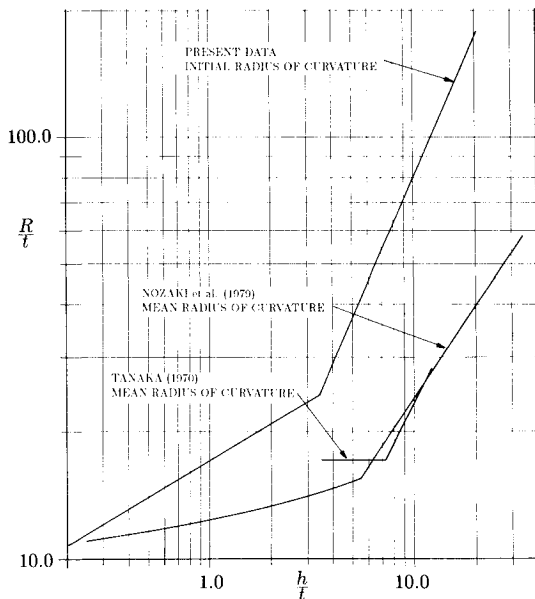


Fig. 10 Jet centerline radius of curvature. The initial radius of curvature is substantially larger than the mean radius of curvature for all but the smallest offset ratios investigated. Measurements due to the previous investigators have been rescaled to be consistent with the present normalizations.

previously assumed.<sup>1-4,6,8</sup> Bourque<sup>7</sup> suspected that the curvature is not constant and consequently, he described the trajectory of the jet as a sinusoid in his theory for the reattachment length and mean cavity pressure. The results of this theory are in better agreement with the data than other theories that assume the jet path to lie on the arc of a circle.

### Conclusions

Variations with offset ratio of the jet exit transverse pressure difference, reattachment wall static pressure distribution, cavity length, and mass flow augmentation have been determined experimentally for the range  $0.194 \leq h/t \leq 21.3$ . The experimental data have been used to provide heuristic relations, defined in two segments, which give the jet exit transverse pressure difference as a function of the offset ratio. For large offset ratios, the exit transverse pressure difference scales closely to the inverse of the offset ratio, as predicted by dimensional analysis. Except for the lowest offset

ratios, the pressure difference across the jet at the exit station was found to be significantly less than the average pressure difference across the jet acting over the length of the cavity. As a consequence of this, the initial radius of curvature of the jet centerline is significantly larger than the mean radius of curvature, and thus the trajectory of the jet may not be well represented by the arc of a circle.

The cavity length measurements agree with those published by previous investigators. In agreement with dimensional analysis, it was found that as the offset ratio becomes large compared to unity,  $x_r/h$  approaches a constant, whose value has been determined to be 1.25. Prediction of the mass flow augmentation, based on knowledge of the exit transverse pressure difference, is in good agreement with the measured values. Thrust augmentation is predicted to exist for offset ratios of less than one half. This conclusion suggests that both interfering and reattaching jets can be used to improve the performance of their free jet counterparts.

### Acknowledgment

This research was funded by NASA Grant NCC 2-150.

### References

- <sup>1</sup>Sawyer, R. A., "The Flow Due to a Two-Dimensional Jet Issuing Parallel to a Flat Plate," *Journal of Fluid Mechanics*, Vol. 9, May 1960, pp. 543-561.
- <sup>2</sup>Bourque, C. and Newman, B. G., "Reattachment of a Two-Dimensional Incompressible Jet to an Adjacent Flat Plate," *Aeronautical Quarterly*, Vol. 11, Aug. 1960, pp. 201-232.
- <sup>3</sup>Newman, B. G., "The Deflection of Plane Jets by Adjacent Boundaries-Coanda Effect," *Boundary Layer and Flow Control*, Vol. 1, edited by G. V. Lachmann, Pergamon Press, Oxford, England, 1961, pp. 232-264.
- <sup>4</sup>Sawyer, R. A., "Two-Dimensional Reattaching Flows Including the Effects of Curvature on Entrainment," *Journal of Fluid Mechanics*, Vol. 17, Dec. 1963, pp. 481-498.
- <sup>5</sup>Rodrigue, G., "Recollement d'un Jet Incompressible a une Paroi Adjacente avec Injection dans la Bulle de Separation," Ph.D. Thesis, Laval University, Quebec, Canada, 1966.
- <sup>6</sup>McRee, D. I. and Moses, H. L., "The Effect of Aspect Ratio and Offset on Nozzle Flow and Jet Reattachment," *Advances in Fluidics*, edited by F.T. Brown, ASME Press, New York, 1967, pp. 142-161.
- <sup>7</sup>Bourque, C., "Reattachment of a Two-Dimensional Jet to an Adjacent Flat Plate," *Advances in Fluidics*, edited by F. T. Brown, ASME Press, New York, 1967, pp. 192-204.
- <sup>8</sup>Perry, C. C., "Two-Dimensional Jet Attachment," *Advances in Fluidics*, edited by F. T. Brown, ASME Press, New York, 1967, pp. 205-217.
- <sup>9</sup>Kumada, M., Mabuchi, I., and Oyakawa, K., "Studies on Heat Transfer to Turbulent Jets with Adjacent Boundaries," *Bulletin of the JSME*, Vol. 16, Nov. 1973, pp. 1712-1722.
- <sup>10</sup>Nozaki, T., Hatta, K., Nakashima, M., and Matsumura, H., "Reattachment Flow Issuing from a Finite Width Nozzle," Rept. 1, *Bulletin of the JSME*, Vol. 22, March 1979, pp. 340-347.
- <sup>11</sup>Nozaki, T., Hatta, K., Sato, N., and Matsumura, H., "Reattachment Flow Issuing from a Finite Width Nozzle," Rept. 2, *Bulletin of the JSME*, Vol. 24, Feb. 1981, pp. 363-369.
- <sup>12</sup>Shakouchi, T. and Kuzuhara, S., "Analysis of a Jet Attaching to an Offset Parallel Plate," *Bulletin of the JSME*, Vol. 25, May 1982, pp. 766-773.
- <sup>13</sup>Nozaki, T., "Reattachment Flow Issuing from a Finite Width Nozzle," Rept. 4, *Bulletin of the JSME*, Vol. 26, Nov. 1983, pp. 1884-1890.
- <sup>14</sup>Miller, D. R. and Comings, E. W., "Force-Momentum Fields in a Dual-Jet Flow," *Journal of Fluid Mechanics*, Vol. 7, Feb. 1960, pp. 237-256.
- <sup>15</sup>Tanaka, E., "The Interference of Two-Dimensional Parallel Jets," Rept. 1, *Bulletin of the JSME*, Vol. 13, No. 56, 1970, pp. 272-280.
- <sup>16</sup>Tanaka, E., "The Interference of Two-Dimensional Parallel Jets," Rept. 2, *Bulletin of the JSME*, Vol. 17, July 1974, pp. 920-927.
- <sup>17</sup>Marsters, G. F., "Interaction of Two Plane, Parallel Jets," *AIAA Journal*, Vol. 15, Dec. 1977, pp. 1756-1762.
- <sup>18</sup>Van Dyke, M., "Higher-Order Boundary-Layer Theory," *Annual Review of Fluid Mechanics*, edited by M. van Dyke, Parabolic Press, Stanford, CA, 1969, pp. 265-292.